communications biology

A Nature Portfolio journal

Article

https://doi.org/10.1038/s42003-025-07990-4

Single-cell transcriptional responses of T cells during microsporidia infection

Yunlin Tang[1,2], Lu Cao[1,2], Jiangyan Jin[1,2], Tangxin Li[1,2], Yebo Chen[1,2], Yishan Lu[1,2], Tian Li[1,2], Louis M. Weiss[3,4], Guoqing Pan[1,2], Jialing Bao[1,2,6] ✉ & Zeyang Zhou[1,2,5,6] ✉

T cells have been reported to play critical roles in preventing of microsporidia dissemination. However, there roles and functions of each subset remain unclear. Here in the study, we performed a thorough analysis of murine splenic T-cell response analysis via single-cell RNA sequencing during microsporidia *E. cuniculi* infection. We demonstrated that Type I T helper (Th1) cells, T follicular helper (Tfh) cells, effector CD8 + T cells and proliferating CD8 + T cells were activated and expanded after infection. Activated Th1 cells and Tfh cells presented significantly upregulated gene expression of *Ifng* and *Il21*, respectively. A subcluster of Th1 cells with high *Csf1* expression was detected after infection. Subsets of activated CD8 + T cells were markedly enriched with high expression of cytotoxic-function related genes such as *Gzma* and *Gzmb*, whereas some active CD8 T cells were enriched with proliferation-function related genes *Mki67* and *Stmn1*. Other subsets of T cells including NK T cells, Myb+ T cells, γδ T cells and Cxcr6+ T cells, were also analyzed in this study yet no expansion was observed. In summary, our findings provide in-depth and comprehensive insights into T-cell responses during microsporidia infection, which will be valuable for further investigations.

Microsporidia are a large group of obligate intracellular pathogens with a uniquely polar-tube-related invasion mechanism to host cells[1,2]. These pathogens can infect a broad range of hosts from invertebrates to vertebrates including humans through horizontal and vertical transmission[3–5]. Microsporidia infection may manifest as a long-term subclinical condition in immunocompetent individuals but can cause clinical diseases in immunocompromised individuals, especially in cases of HIV infection, organ transplantation, chemotherapy, and advanced age[6–10]. The bias in microsporidia infection manifestations across different immune conditions highlights the crucial role of immune competence in controlling microsporidia dissemination in the host.

Both innate and adaptive immune responses play important roles in protecting host from microsporidia infection[11]. Toll-like receptors (TLRs) in innate immune cells may recognize *Encephalitozoon cuniculi*[12,13]. Macrophages can be activated by *E. cuniculi* and *E. intestinalis* through TLR2 to produce inflammatory cytokines including TNFα and IL8[12]. Dendritic cells (DCs) can recognize *E. cuniculi* by TLR4 and express IL12 and IFNγ to prime the optimal CD8 + T-cellresponse[13–15]. Interestingly, T cells especially CD8 + T cells, play crucial roles in preventing microsporidia dissemination. *CD8*−/− mice and *Perforin*−/− mice are more susceptible to microsporidia infection and dissemination in vivo[16,17]. Adaptive transfer of CD8 + T cells from immunocompetent individuals can abolish the effects of lethal challenge with microsporidia in severe combined immunodeficiency (SCID) mice lacking T cells and B cells[18]. CD8 + T cells exhibit polyfunctional abilities including cytotoxic responses and cytokines secretion, during microsporidia infection[17]. A subset of KLRG1 + CD8 + T cells can be activated and produce granzyme B, IFNγ and TNFα under the facilitation of IL21 secretion by CD4 + T cells[19,20]. CD4 + T cells can produce IFNγ and IL21 during microsporidia infection[20,21]. However, the role of CD4 + T cells in the induction of the CD8 + T-cell response against microsporidia is underappreciated as the depletion of CD4 + T cells does not abolish the response of CD8 + T cells and their ability to control microsporidia dissemination[21]. Considering the heterogeneity of T cells, a comprehensive and in-depth understanding of the responses of various subsets of T cells during microsporidia infection is needed.

Single-cell RNA sequencing (scRNA-seq) is a powerful approach for revealing the heterogeneity of immune cells during infection, enabling the discovery of novel immune cell subsets, identifying specific cell markers for distinct subsets, and profiling the gene expression patterns within these subsets[22–25]. However, to the best of our knowledge, few studies have applied scRNA-seq to investigate the gene expression profiles of host immune cells during microsporidia infection.

[1]State Key Laboratory of Resource Insects, Southwest University, Chongqing, China. [2]Chongqing Key Laboratory of Microsporidia Infection and Control, Southwest University, Chongqing, China. [3]Department of Pathology, Albert Einstein College of Medicine, New York, NY, USA. [4]Department of Medicine, Albert Einstein College of Medicine, New York, NY, USA. [5]College of Life Sciences, Chongqing Normal University, Chongqing, China. [6]These authors jointly supervised this work: Jialing Bao, Zeyang Zhou. ✉e-mail: baojl@swu.edu.cn; zyzhou@swu.edu.cn

Currently, we have performed single-cell RNA sequencing (scRNA-seq) on splenic T cells isolated from microsporidia infected and control mice to gain comprehensive insight into T-cell responses during microsporidia infection. In our study, we identified a broad range of T-cell subsets and analyzed differentially expressed genes (DEGs) related to these subsets. Our research generated a high-resolution landscape of mouse splenic T cells during microsporidia infection, providing valuable insights into the immune responses to this group of unicellular and intracellular parasites.

Results

scRNA-seq profiling of splenic T cells after *E. cuniculi* infection

To comprehensively analyze the immune response of T cells during *E. cuniculi* infection, we performed droplet-based scRNA-seq on mouse splenic T cells isolated from *E. cuniculi*-infected (14 dpi) and uninfected control (Ctrl) mice. After the cell preparation procedures, a total of 2×10^4 cells/group were subjected to single-cell 3′ RNA-sequencing. A cell filter was applied during the analysis, and consequently, 6819 cells (Ec group) and 6604 cells (control group) passed the filter and underwent sequencing. *Cd3e*, *Cd3d*, and *Cd3g* expression was used as markers to further validate the findings in T cells. As a result, 6413T cells from the Ec group and 6297T cells from the control group (12,710 total cells) were validated and ready for further analysis. All these validated T cells were distributed across 16 cell clusters and visualized with uniform manifold approximation and projection (UMAP) (Fig. 1A). Based on the expression of canonical and selected marker genes (Table S1), the 16 cell clusters were annotated as naïve CD8 + T cells (CD8 Naïve, C1), double-negative/positive T cells (DN/P T cells, C2), effector CD8 + T cells (CD8 Effector, C3), follicular helper CD4 + T cells (CD4 Tfh, C4), effector CD4 + T cells (CD4 Effector, C5), proliferating CD8 + T cells (CD8 Proliferating, C6), naïve CD4 + T cells (CD4 Naïve, C7), natural killer T cells (NK T cells, C8), Myb + T cells (C9), Cela2a + CD8 + T cells (CD8 Cela2a + , C10), Regulatory CD4 + T cells (Treg, C11), Cxcr6 + T cells (C12), memory CD8 + T cells (CD8 Memory, C13), Ifit1 + CD8 + T cells (CD8 Ifit1 + , C14), Nr4a1 + CD8 + T cells (CD8 Nr4a1 + , C15) and γδ T cells (C16) (Fig. 1B). Among these, the naïve cell subsets including the CD4 Naïve, CD8 Naïve and DN/P T cells, were predominant in the Ctrl group and decreased in the Ec group, whereas the effector cell subsets, including CD4 Effector, CD4 Tfh and CD8 Effector, were significantly expanded (Figs. 1C and S1). The CD4 Effector accounted for only 1.1% of the T cells in the uninfected mice but increased to 12.7% after *E. cuniculi* infection. Additionally, the proportion of CD8 Effector changed from 1.4% to 23.1% following *E. cuniculi* infection (Fig. 1C). Intriguingly, the subset of CD8 Proliferating expressing cell cycle related

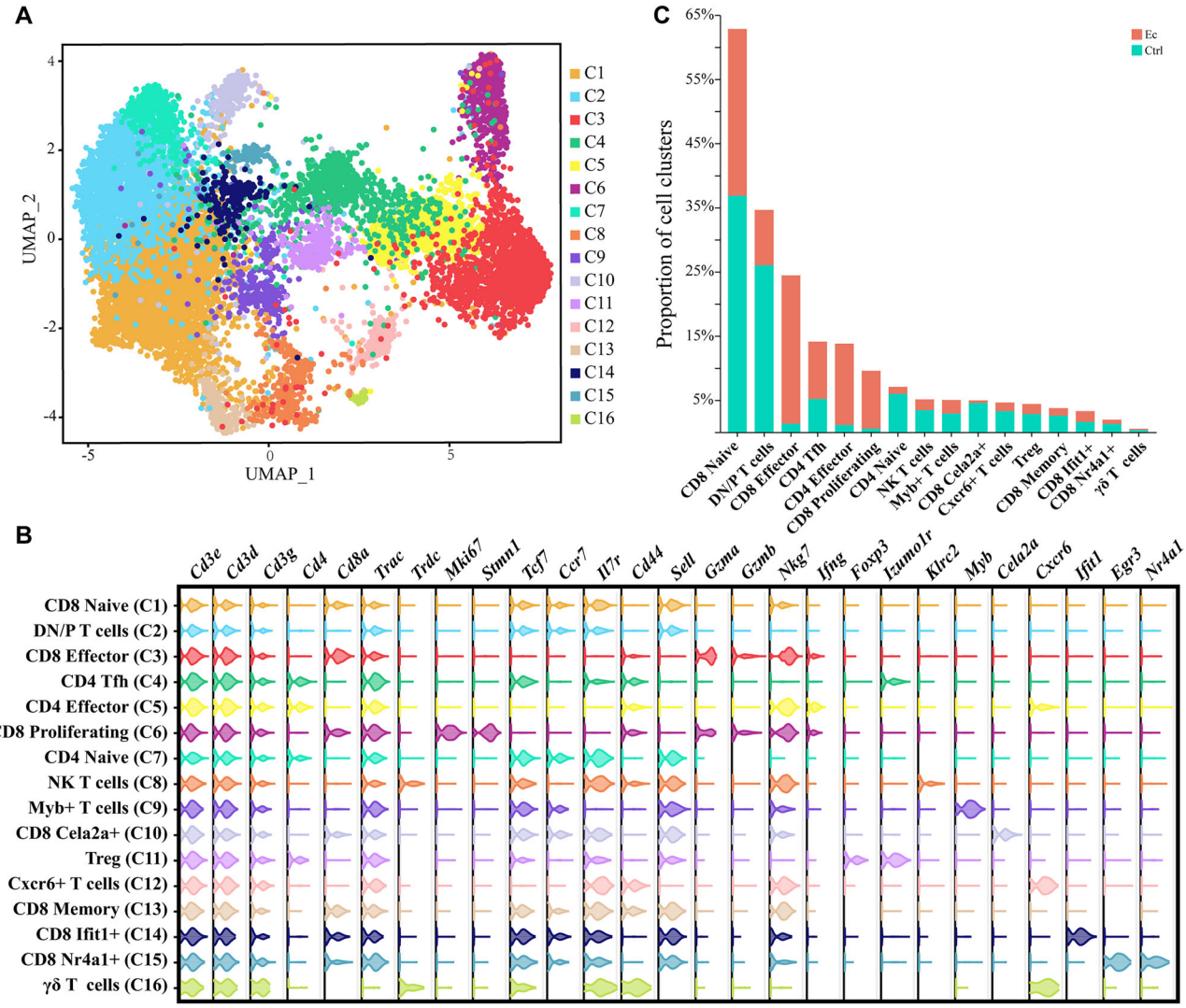

Fig. 1 | Single-cell transcriptional landscape of T cells during microsporidia infection. A UMAP plots of all T cells in the global analysis. Sixteen cell clusters were obtained from approximately 12710 valid T cells. The cells are colored according to their cell clusters. **B** Normalized expression of cell marker genes used to annotate the 16 clusters of T cells. The columns represent selected marker genes, and the rows represent clusters with the same color in (**A**). **C** Proportion of T-cell subsets in the Ctrl and Ec groups.

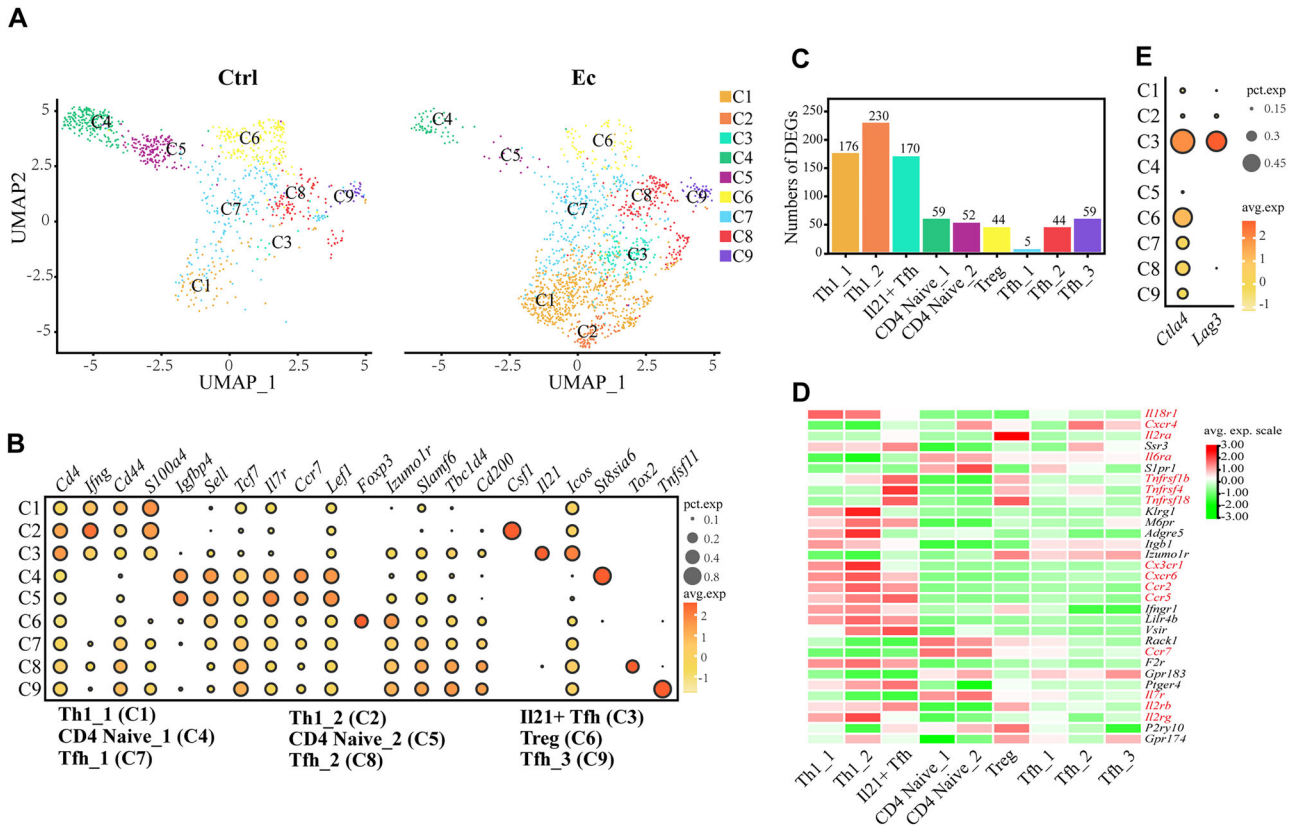

Fig. 2 | Subcluster analysis of CD4 + T cells. A UMAP of CD4 + T-cell subclusters. Eight cell subclusters were identified in the Ctrl group, and 9 cell subclusters were identified in the Ec group. The points are colored according to the cell subclusters. **B** Average expression (color scale) and percent expression (size scale) of marker genes used to annotate the CD4 + T-cell subclusters. The columns represent selected marker genes, and the rows represent subclusters. **C** Number of DEGs across CD4 + T-cell subclusters. **D** Receptor genes (rows) that were differentially expressed across CD4 + T-cell subclusters (columns). Red: high expression; green: low expression. Selected genes are highlighted. **E** Average expression (color scale) and percent expression (size scale) of selected genes related to T-cell exhaustion in CD4 + T-cell subclusters.

genes, including *Mki67* and *Stmn1*, which are reported to have proliferation functions[26,27], was markedly increased in the Ec group (Figs. 1B, C and S1A). These results suggest that *E. cuniculi* infection can induce immune responses in both CD4 + T cells and CD8 + T cells, that the activated CD4 + T-cell subsets are diverse, and that activated CD8 + T cells exhibited the capacity of proliferation in spleen.

CD4 + T-cell responses during *E. cuniculi* infection

Recluster analysis of CD4 + T cells was conducted and nine subclusters were obtained, among which a unique subcluster (C2) was found in the Ec group but not in the Ctrl group (Fig. 2A). According to cluster-specific gene expression, two subclusters (C1 and C2) were identified as Type I helper T cells (Th1_1 and Th1_2), which highly expressed *Ifng* and were distinguished by the specific expression of *Csf1* in Th1_2. Two subclusters (C4 and C5) highly expressing *Tcf7*, *Il7r*, *Ccr7*, *Lef1*, and *Sell* were annotated as naïve CD4 + T cells (CD4 Naïve_1 and CD4 Naïve_2). Four subclusters (C3, C7, C8, and C9) were annotated as follicular helper CD4 + T cells (Il21+ Tfh, Tfh_1, Tfh_2, and Tfh_3) with the expression of *Icos*, *Izumo1r*, and *Cd200*[28–30], and one subset of Tregs (C6) was recognized with the expression of *Foxp3* (Fig. 2B). Among these subsets, naïve CD4 + T-cell and Treg cell subsets decreased after infection, whereas Th1_1, Th1_2 and IL21+Tfh increased. Th1_1 was the most abundant and accounted for approximately 42% of the CD4 + T cells in the Ec group and 8% of the CD4 + T cells in the Ctrl group, and the specific Th1_2 accounted for about 7% of the CD4 + T cells in the Ec group. Within the Tfh subcluster, the proportion of Il21 + Tfh increased from 0.9% to 7.1%, while the proportions of the remaining subclusters were almost unchanged after infection (Figs. 2A and S2A).

To identify the specific functions of each CD4 + T-cell subset, we performed DEG analysis of each specific subset compared with the remaining subsets (Fig. 2C). We observed that the Th1_1, Th1_2, and Il21+ Tfh subclusters harbored more than 150 DEGs. Among the DEGs, the expression patterns of the receptor genes were similar between Th1_ 1 and Th1_2, of which genes of cytokine and chemokine receptors, including *Ifngr1*, *Il2b*, *Cx3cr1*, *Il18r1*, *Il2g*, *Tnfrsf1b*, and *Ccr2*, were highly expressed in Th1_1 and Th1_2 (Fig. 2D). Additionally, *Klrg1*, which encodes an inhibitory receptor involved in both innate and adaptive immune responses, was specifically expressed in Th1_1 and Th1_2. The expression of *Ccr5* and *Cxcr6* was significantly upregulated in Th1_1, Th1_2, and Il21+ Tfh. *Tnfrsf1b*, *Tnfrsf18*, and *Tnfrsf4* were highly expressed in Il21+Tfh but expressed at low levels in the remaining Tfh subsets. Among these remaining Tfh subsets, there were limited upregulated receptor genes, except for *Izumo1r*. The highly expressed receptor genes of Treg included *Izumo1r*, *Il2ra*, and *Tnfrsg18*, and naïve CD4 + T-cell subsets markedly expressed *Il6r*, *Ccr7*, and *Il7r*. In addition, genes encoding cell exhaustion-related membrane proteins in CD4 + T cells were identified (Fig. 2E). Especially in the IL21+ Tfh subset, which highly expresses *Ctla4* and *Lag3*. These two genes were upregulated in CD4 + T cells under infection conditions (Fig. S2B and Supplementary Data 1). The differential expression of these receptor and membrane protein genes suggested potential and specific activation mechanisms and roles for specific CD4 + T-cell subsets.

In the current study, Th1_2 was found to express *Ifng* and *Csf1* simultaneously. To determine the differences between Th1_1 and Th1_2, we compared the gene expression profiles of the two Th1 subsets (Figs. 3A and S3). Th1_1 exhibited upregulated expression of *Tcf7*, which regulates T-cell development and response[31–33]; *Zc3h15*, which is reported to

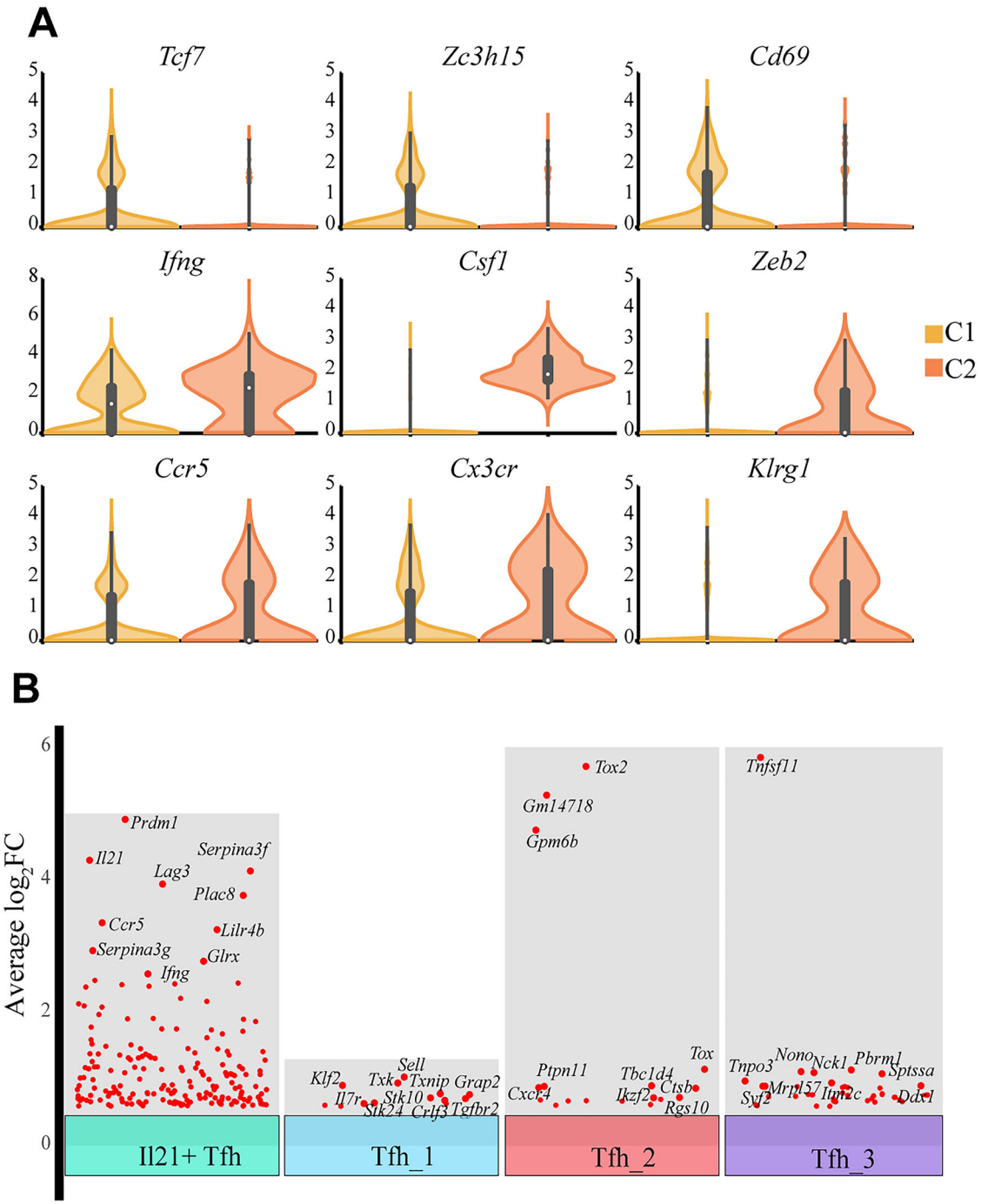

Fig. 3 | Comparative analysis of CD4 + T-cell subclusters. A Normalized expression levels of selected genes differentially expressed between Th1_1 and Th1_2. **B** Upregulated gene analysis across all Tfh subclusters.

modulate cell proliferation[34]; and *Cd69*, which is rapidly expressed in lymphocytes after activation[35]. Th1_2 was a unique subcluster in the Ec group and presented increased expression of *Ifng*, *Csf1*, *Zeb2*, *Ccr5*, *Cx3cr*, and *Klrg1*. *Csf1* encodes MCSF1, which is a primary factor for macrophage differentiation, survival, and proliferation. This bias of gene expression indicated that Th1_2 and Th1_1 may represent distinct subclusters of helper T cells.

DEG analysis within the Tfh subsets revealed that IL21+ Tfh presented the greatest number of upregulated genes, whereas the other three subsets presented fewer upregulated genes, especially those with significant fold changes (Fig. 3B). *Il21* and *Ifng* were markedly highly expressed in IL21+ Tfh. TOX2, which are reported to drive T follicular helper cells (Tfh) development[36], exhibited a high level of gene expression in Tfh_2. *Tnfsf11* expression was marked in Tfh_3 (Figs. 2B and 3B). The increased proportion after infection and differences in gene expression with Tfh cells implied that Tfh cells may be activated to play multiple roles in preventing microsporidia infection.

CD8 + T-cell responses associated with *E. cuniculi* infection

CD8 + T cells are critical effector cells in protection against microsporidia infection with polyfunctional responses, particularly cytotoxic responses[16,19]. In current study, we identified seven clusters of CD8 + T cells, including CD8 Effector and CD8 Proliferating, which highly expressed granzyme genes (*Gzma* and *Gzmb*) and were markedly expanded in the Ec group

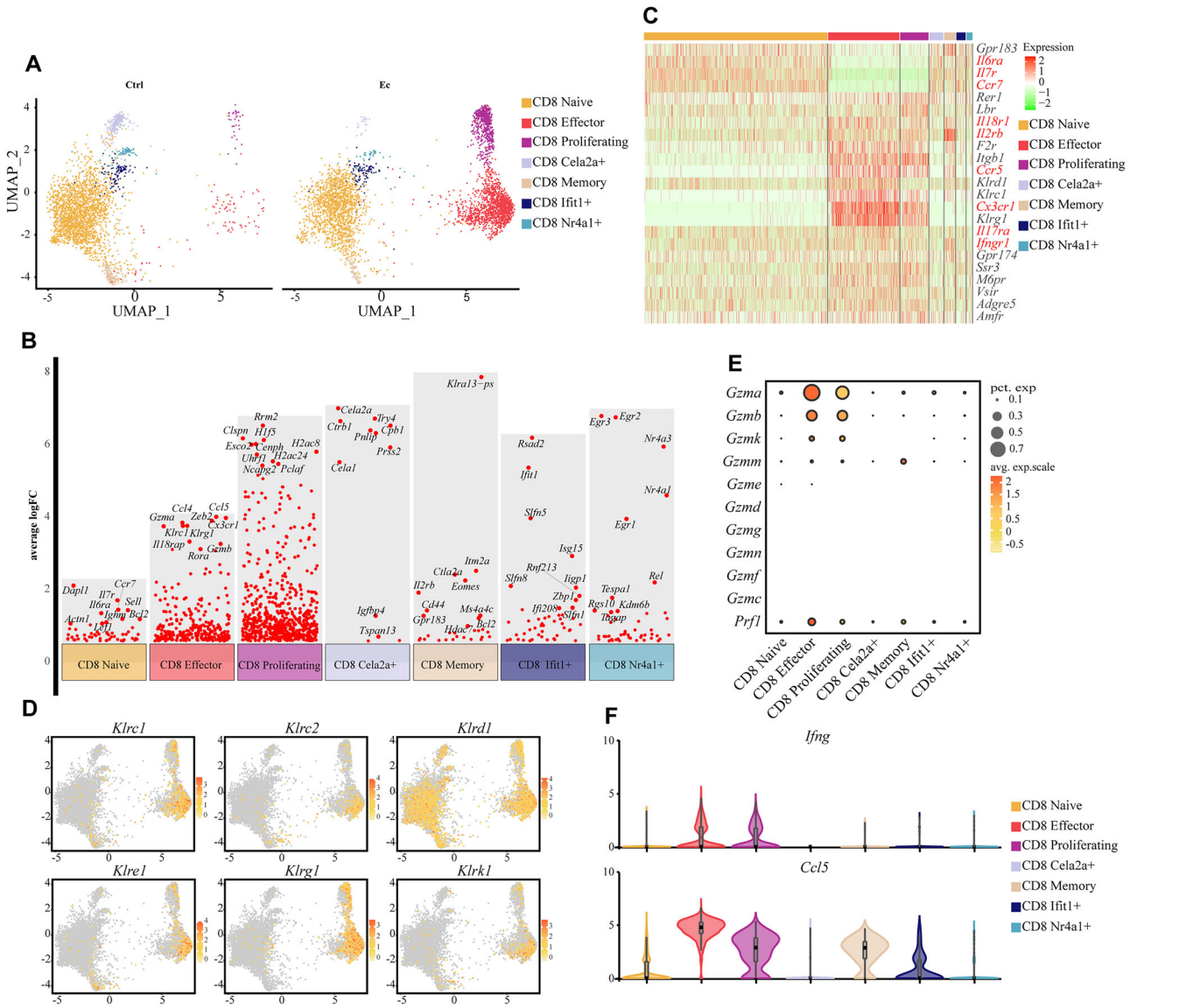

Fig. 4 | Transcriptional analysis of CD8 + T-cell clusters. A UMAP plots of CD8 + T-cell clusters. Seven cell subclusters were identified in the Ctrl and Ec groups. The points are colored according to the cell subclusters. **B** Upregulated gene analysis across all CD8 + T-cell clusters. **C** Receptor genes (rows) that were differentially expressed across CD8 + T-cell clusters (columns). Red: high expression; green: low expression. The selected genes are highlighted. **D** Normalized expression levels of genes related to KLRs in CD8 + T cells. **E** Average expression (color scale) and percent expression (size scale) of selected genes related to the cytotoxic response in CD8 + T-cell subclusters. **F** Normalized expression levels of *Ifng* and *Ccl5* differentially expressed across all CD8 + T-cell clusters.

(Figs. 1C and 4A). CD8 Naïve, CD8 Cela2a+, CD8 Nr4a1+ and CD8 Memory were decreased in the infected group. To investigate transcription in CD8 + T cells during *E. cuniculi* infection, we comparatively analyzed the gene expression of seven subsets. Both CD8 Effector and CD8 Proliferating were markedly transcriptionally active, whereas CD8 Cela2a+ and CD8 Memory were the least activated (Fig. 4B). The increased proportion and number of DEGs in CD8 Effector and CD8 Proliferating demonstrated that these two subsets were activated by *E. cuniculi* infection.

Among the DEGs, we first analyzed the receptor gene expression of CD8 + T cells, and found that the upregulated receptor genes were similar between CD8 Effector and CD8 Proliferating (Fig. 4C). Genes encoding cytokine and chemokine receptors including *Il18r1*, *Il2rb*, *Ccr5*, and *Cx3cr1*, were upregulated and highly expressed in activated subsets (Fig. 4C). However, *Il18r1*, *Cx3cr1*, and *Il17ra* were significantly upregulated in CD8 Effector compared to CD8 Proliferating (Fig. S4). CD8 Naïve markedly expressed *Gpr183*, *Il6ra*, *Il7r*, and *Ccr7*, whereas the other subsets presented limited expression of receptor genes (Fig. 4C). CD8 + T-cell activation during microsporidia infection requires various cytokines and chemokines[17]. The upregulated expression of cytokine and chemokine receptor genes may provide valuable insights into the roles of these signaling molecules in promoting the response of CD8 + T cells during microsporidia infection. Moreover, genes encoding killer cell lectin-like receptors (KLRs), including *Klrc1*, *Klrc2*, *Klre1*, *Klrg1*, and *Klrk1*, showed moderate expression in activated CD8 + T cells, and *klrd1* was widely expressed in most CD8 + T cells (Fig. 4D). CD8 + T cells expressing the inhibitory receptor KLRG1 play an essential role in protecting the host from microsporidia infection[20], but the specific roles of other KLRs+CD8 + T cells against microsporidia are still not fully understood.

The cytotoxic T lymphocyte response of CD8 + T cells, including the upregulation of granzyme B, was reported to be critical in protecting the host during microsporidia infection[19]. We found that *Gzma*, *Gzmb* and *Gzmk* were expressed in activated CD8 + T cells, with higher expression in CD8 Effector than in CD8 Proliferating (Fig. 4E). The expression level of *Gzma* was the highest, while that of *Gzmk* was very low. Moreover, *Ifng* was expressed by activated cells, and Ccl5 was expressed in several CD8+ subsets (Fig. 4F). These results indicate that these effector molecules

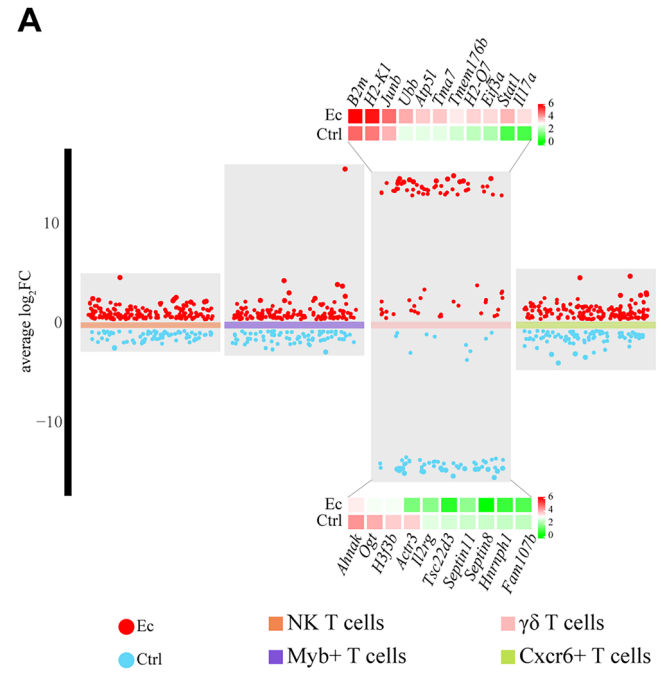

Fig. 5 | Differential gene expression analysis of unconventional T cells. **A** Upregulated and downregulated genes between the Ec and Ctrl groups across unconventional T clusters. The expression levels of selected DEGs in γδ T cells are presented by heatmaps.

involved in the cytotoxic response during microsporidia infection are not limited to GZMB alone, but include GZMA and GZMK. Moreover, these findings confirmed that CD8 + T cells exhibit polyfunctionality during microsporidia infection.

Unconventional T-cell response

In this study, four subsets of unconventional T cells, including NK T cells, Myb+ T cells, γδ T cells and Cxcr6+ T cells, were identified, and none of them showed expansion (Fig. 1B). We compared the gene expression of these subsets between the Ec and Ctrl conditions (Fig. 5A). A few DEGs with significant fold changes were found in NK T cells, Myb+ T cells and Cxcr6+ T cells, and *Gzma* was markedly upregulated in Myb+ T cells in Ec. Several genes with marked fold changes were identified in γδ T cells, including *B2m*, *H2-K1*, *H2-Q7*, *Junb*, and *Il17a*, under infection conditions (Fig. 5). *B2m*, *H2-K1*, and *H2-Q7* are related to major histocompatibility complex class I (MHC I), indicating that *E. cuniculi* may target γδ T cells directly.

Discussion

Previous reports have demonstrated that microsporidia activate vigorous T-cell responses on Day 14 post infection[17,20,37]. However, comprehensive insight into the responses of specific T-cell subsets is still lacking. In this study, we performed scRNA-seq to profile the transcriptional landscape of mouse splenic T cells on Day 14 after microsporidia infection. Consistent with previous reports, we found that effector T-cell clusters, including CD4 Effector, CD4 Tfh and CD8 Effector, were activated and increased in the spleens of mice infected i.p. with *E. cuniculi*. Furthermore, we identified a specific cell cluster, proliferating CD8 + T cells, that exhibited significant expression of genes associated with cell proliferation and underwent marked expansion during microsporidia infection. *Ifng* and *Ccl5* were expressed by activated T cells, *Il21* was expressed only by a subset of CD4 Tfh (Fig. S2C). The main effector molecules of the cytotoxic response expressed by microsporidia-activated CD8 + T cells were GZMA and GZMB. Notably, GZMA presented a higher level of gene expression than GZMB.

CD4 + T cells are heterogeneous and can differentiate into multiple subsets, including Th1, Th2, Th9, Th17, Treg, and Tfh, based on gene expression associated with membrane molecules, transcription factors, and cytokines[38,39]. Although the depletion of CD4 + T cells does not affect the clearance of microsporidia, CD4 + T cells are activated to secrete IFNγ and IL-21 during infection[20,21]. We demonstrated by scRNA-seq that IL21 was produced exclusively in a certain subcluster of Tfh cells identified as Il21+ Tfh, while *Ifng* was expressed in both Th1 cells and Tfh cells. These findings were validated at various scales (Figs. S5 and S6). Our data are consistent with those of previous reports, indicating that microsporidia infection activates the response of Th1 cells and Tfh cells.

Intriguingly, we identified two subclusters of Th1 cells, namely, Th1_1 and Th1_2. Th1_2, a subcluster of Th1 cells with high expression of *Csf1*, was first identified during microsporidia infection. MCSF, which is encoded by *Csf1*, plays important roles in macrophage differentiation, survival, mobilization and proliferation. As reported, MCSF can be produced by multiple cells including endothelial cells, fibroblasts and T cells, under homeostatic and inflammatory conditions[40–43]. Despite the wide range of MCSF-producing cells, specific depletion of MCSF in CD4 + T cells can decrease the activation and proliferation of a certain subset of CD169+ macrophages. Ultimately, this disruption can affect the control of parasite load and impede host recovery following *Plasmodium* parasite infection[42]. Macrophages can recognize microsporidia through TLR2 and produce reactive nitrogen species and reactive oxygen species to control microsporidia[12,44]. Additionally, our previous study demonstrated that microsporidia infection facilitates the maturation of monocytes in bone marrow and promotes their extravasation from peripheral blood[45]. Based on these reports, we hypothesize that MCSF expressed by CD4 + T cells may play a critical role in promoting the macrophage response to microsporidia infection. In addition to *Csf1*, Th1_2 presented DEGs with higher expression than that in Th1_1. IFNγ is a critical effector in the host response against microsporidia and can promote myeloid progenitor migration into the spleen during *Plasmodium* infection[46–48], and ZEB2 is a multi-zinc-finger transcription factor that promotes the terminal differentiation of KLRG1 + CD8 + T cells[49]. The high expression levels of *Ifng* and *Zeb2* indicated that Th1_2 may present a terminal Th1 cell subcluster compared with Th1_1. The bias in gene expression provides potential approaches to illustrate the differences in these two Th1 subclusters during microsporidia infection.

CD8 + T cells play a critical role in controlling intracellular pathogen dissemination through the death receptor pathway or granule exocytosis pathway. Previous studies revealed that GZMB and CD95L(FasL) expression was upregulated in CD8 + T cells after microsporidia infection[15,19]. Unexpectedly, we found that *Gzma* showed a notable expression in activated CD8 + T cells. The proportion of cells expressing *Gzma* was higher than the proportion of cells expressing *Gzmb* (Fig. 4E). CD8 + T cells have the potential to express both GZMA and GZMB simultaneously but occasionally express only one of these molecules depending on the specific stimulation that they encounter[50,51]. In our study, high expression of GZMA was demonstrated not only by scRNA-seq analysis but also by flow cytometry (Fig. S6B). GZMA can trigger pyroptosis, which is distinct from apoptosis induced by GZMB[52–54]. The diverse expression of cytotoxic molecules suggested that infected cells may express multiple molecules to induce polyfunctional immune responses during microsporidia infection.

In addition to αβ T cells, γδ T cells perform essential and polyfunctional roles in controlling pathogen infection, including *plasmodium*, West Nile virus, as well as microsporidia[37,55,56]. During microsporidia infection, IFNγ derived from γδ T cells is crucial for facilitating CD8 + T-cell response. The absence of γδ T cells increases susceptibility to infection by these pathogens[37]. In this study, *Trdc* and *Trgc*, which are related to TCR γδ, were expressed in two clusters including NK T cells and γδ T cells. The majority of NK T cells express αβ TCR, and a small portion of NK T cells express γδ TCR; however, researchers sometimes find it difficult to distinguish these two receptors types of NK T cells, strictly[57]. For γδ T cells, comprehensive and transcriptional analysis is usually difficult because of the extremely small portion of γδ T cells among other cells. Therefore, performing comprehensive studies to assess γδ T-cell responses at single-cell resolution would be highly valuable. In this way, we would be able to

gain insights into the specific immune responses mediated by γδ T cells and their roles in combating microsporidia. Related studies could promote the development of targeted therapeutic strategies for microsporidiosis in vulnerable populations, particularly in HIV patients with low CD4 T-cell counts[7,58]. Given these valuable findings, the limitations of this study should also be noted. In this study microsporidia infection was established by i.p. injection, which is different from natural infection through the digestive tract. Comparative analyses of immune responses among different modes of infection should be taken into consideration, as specific modes of microsporidia infection may lead to distinct consequences[59,60].The limited number of time points in the experiments restricts the amount of detailed and available information about the activation, differentiation, and proliferation of specific T-cell subsets. To obtain a more comprehensive understanding of these processes, it would be valuable to expand the number of time points during the experimental design. In our study, the cells were isolated and combined from five mice in each group. Although it's not unusual for single-cell RNA sequencing that cells were pooled and combined from three to eight mice per group, as long as the variations among individual animals were highly controlled[61–63]. We have to admit the limitations of pooled samples in a single-cell transcriptomics analysis, such as the impact of pool size, multiplexing accuracy and sequencing coverages. To minimize these impacts, we strictly controlled the experiment manipulations and made sure all individual mice, either in infection or control group, were in the same state. Next, we conducted qPCR and ELISA assays and verified that the pathogen loads and host immune responses were comparable among individuals (Fig. S7B and D). To optimize the sequence coverage, we used as much as cells (about 10^6 cells/mL) for the generation of single-cell 3' RNA-seq libraries. Based on the above, we tried the best to minimize the impacts and the limitations pooled samples for this assay. Additionally, while our transcriptomic data identified key transcriptional changes in T cells during microsporidia infection, further experimental validations may be needed. In fact, we have verified the responses of various T-cell subsets, such as CD8 + T cells—the expression of GZMA by flow cytometry assay (Fig. S6B), as well as the responses of CD4 + T cells—the expressions of IL21 by Western blot assay (Fig. S6C). More validating experiments such as specific T cell subsets transferring into immunodeficient mice and cytokine profiling analysis assays could be conducted to fully elucidate the T cell immune response. Comparative and comprehensive analyses of immune responses following infection with different microsporidia species are needed in future research.

Methods

Animals and microsporidia infection

Eight-week-old female C57BL/6J mice were acquired from Hunan SJA Laboratory Animal (Hunan, China) and reared under pathogen-free conditions. The Institutional Animal Care and Use Committee of Southwest University (IACUC-20230524-01) approved all animal experiments performed in this study. We have complied with all relevant ethical regulations for animal use. *E. cuniculi* (ATCC PRA-336) were a gift from Prof. Louis Weiss (Albert Einstein College of Medicine, New York, USA) and were reproduced in rabbit kidney cells (RK13, ATCC CCL-37). RK-13 cells were maintained in RPMI 1640 (Gibco, USA) supplemented with 10% fetal bovine serum (FBS) (Gibco, USA) at 37 °C and 5% CO_2. The spores were obtained from the culture supernatant. Briefly, the culture supernatant was collected, concentrated by centrifugation, and resuspended in PBS before being passed through a 25-G needle attached to a 5 mL syringe approximately ten times. The syringe-lysed suspension was passed through a filter, centrifuged at 500 × *g* for 10 min and washed with PBS three times. The spore pellets were counted after being washed and centrifuged, and then stored at 4 °C before injection. *E. cuniculi* (Ec) spores resuspended in PBS were injected intraperitoneally (i.p., 2×10^7 spores/mouse, five mice in total) into the mice. The infection loads and host responses among individuals were detected and within comparable ranges (Fig. S7). The control mice (Ctrl, five mice in total) were injected i.p. with an equal volume of PBS.

Cell preparation

On Day 14 post infection, the mice were sacrificed by carbon dioxide narcosis followed by cervical dislocation. The spleens were removed and homogenized through mechanical disruption, resulting in the release of splenocytes. These splenocytes were subsequently strained through a 70 μm filter to obtain a single-cell suspension. About 10^8 splenic cells were isolated from each mouse after red blood cell lysis, and 1×10^7 cells/ mouse from 5 mice were mixed and combined for the next step. The EasySep™ Mouse T Cell Isolation Kit (STEMCELL Technologies, Canada) was used to isolate T cells through immunomagnetic negative selection. Briefly, rat serum and then isolation cocktail were added to the samples. Next, the sample was incubated with RapidSpheres, and a magnet was applied to negatively select T cells. After magnetic selection, 2.7×10^6 cells and 3.3×10^6 cells were isolated from the control and Ec infection groups, respectively. Then, 100 μL of cell suspension (1×10^6 cells/mL) per group was used to generate single-cell 3' RNA-seq libraries.

Single-cell RNA sequencing and data analysis

The cells were prepared and a total of 2×10^4 coated cells/group were loaded into each lane to generate gel beads-in-emulsion in a MobiNova-100 (MobiDrop, China). Single-cell 3′ RNA-seq libraries were generated using MobiCube Single-Cell 3′ RNA-seq Kits (MobiDrop, China). The 3′ RNA-seq libraries were sequenced under a paired-end model on an Illumina NovaSeq 6000 platform. MobiVision (v1.1) was used to analyze the raw single-cell transcriptomic data. The reads were aligned to the *Mus musculus* reference GRCm39, and a filtered cell-gene matrix was obtained.

The cell-gene matrix of each sample was imported to Seurat (v3.1.1) for downstream analysis[64,65]. First, the cell doublets were removed by using the DoubletFinder tool (v2.0.3) following the manufacturer's instructions[66]. Next, cells that met the following criteria were excluded: fewer than 590 or more than 1900 genes, a UMI count greater than 6900, and a mitochondrial UMI percentage higher than 10%. After quality control, the NormalizeData function was used to normalize the gene expression level and the FindVarialbleFeature function was used to calculate the top 2000 variable genes. To reduce dimensions, principal component analysis (PCA) was performed with scale data generated by the ScaleData function. The FindNeighbors and FindClusters functions were used to cluster cells. The cell clusters were visualized via uniform manifold approximation and projection (UMAP). The cell clusters expressing *Cd3e*, *Cd3d*, and *Cd3g* were recognized as T-cell subsets. The dataset of T-cell subsets was selected and integrated with the IntegrateData function, and subsequently reanalyzed for cell clustering[64,65]. The reanalyzed T-cell clusters were annotated based on the cluster-specific marker gene expression (Table S1)[67], including naïve CD4 T cells (*Cd4*, *Sell*), effector CD4 T cells (*Cd4*, *Cd44*), regulatory T cells (*Cd4*, *Foxp3*), follicular helper CD4 + T cells (*Cd4*, *Il21*, *Izumo1r*, *Icos*), naïve CD8 T cells (*Cd8a*, *Sell*), effector CD8 T cells (*Cd8a*, *Cd44*), γδ T cells (*Trdc*), NKT cells (*Nkg7* and *Klrc2*), proliferating cells (*Mki67* and *Stmn1*), γδ T cells (*Trdc*) and others.

Statistics and reproducibility

Statistical analyses were performed using GraphPad Prism, including two-tailed unpaired Student's *t*-tests. $P < 0.05$ was considered significant. Data were presented as mean ± SD. No data were excluded from the analyses.

For scRNA-seq analysis expressed gene (DEG) analysis was performed using the Wilcoxon rank sum test to compare the expression value of each gene within a given cluster against the expression in the remaining cells or specific clusters[68]. Genes with significantly changed expression levels were filtered using a minimum expression percentage of 25% within the given cluster, a minimum fold change of 1.5 and a maximum *p* value of 0.05.

Reporting summary

Further information on research design is available in the Nature Portfolio Reporting Summary linked to this article.

Data availability

The raw sequencing data of this study have been deposited at the Genome Sequence Archive (GSA) of the National Genomics Data Center, Chinese Academy of Sciences (https://ngdc.cncb.ac.cn/gsa, accession number CRA014453) and are accessible. The processed scRNA-seq data reported in this study are openly available from the OMIX, Chinese Academy of Sciences (https://ngdc.cncb.ac.cn/omix, accession number OMIX006892). The uncropped western blot images are available in the Supplementary Information (Supplementary Figs. 8, 9, 10, 11). Differential expression genes (DEGs) of Clusters between Ctrl and Ec are presented in Supplementary Data 1. The source and original data behind graphs are provided in Supplementary Data 2.

Code availability

Data analysis pipeline used in our work follow the MobiDrop instructions and Seurat official websites. The authors declare that all relevant data and custom scripts for analyzing data are available upon reasonable request.

Received: 8 May 2024; Accepted: 24 March 2025;
Published online: 05 April 2025

References

1. Han, B. & Weiss, L. M. Microsporidia: obligate intracellular pathogens within the fungal kingdom. *Microbiol. Spectr.* **5**, https://doi.org/10.1128/microbiolspec.funk-0018-2016 (2017).
2. Han, B. et al. The role of microsporidian polar tube protein 4 (PTP4) in host cell infection. *PLoS Pathog.* **13**, e1006341 (2017).
3. Stentiford, G. D. et al. Microsporidia - emergent pathogens in the global food chain. *Trends Parasitol.* **32**, 336–348 (2016).
4. Dunn, A. M., Terry, R. S. & Smith, J. E. Transovarial transmission in the microsporidia. *Adv. Parasitol.* **48**, 57–100 (2001).
5. Terry, R. S. et al. Widespread vertical transmission and associated host sex-ratio distortion within the eukaryotic phylum Microspora. *Proc. Biol. Sci.* **271**, 1783–1789 (2004).
6. Sak, B., Kváč, M., Kučerová, Z., Květoňová, D. & Saková, K. Latent microsporidial infection in immunocompetent individuals - a longitudinal study. *PLoS Negl. Trop. Dis.* **5**, e1162 (2011).
7. Han, B., Pan, G. & Weiss, L. M. Microsporidiosis in humans. *Clin. Microbiol. Rev.* **34**, (2021). e0001020.
8. Wang, Z. D. et al. Prevalence of *Cryptosporidium*, microsporidia and *Isospora* infection in HIV-infected people: a global systematic review and meta-analysis. *Parasit. Vectors* **11**, 28 (2018).
9. Nagpal, A. et al. Disseminated microsporidiosis in a renal transplant recipient: case report and review of the literature. *Transpl. Infect. Dis.* **15**, 526–532 (2013).
10. Lores, B. et al. Intestinal microsporidiosis due to Enterocytozoon bieneusi in elderly human immunodeficiency virus-negative patients from Vigo, Spain. *Clin. Infect. Dis.* **34**, 918–921 (2002).
11. Moretto, M. M. & Khan, I. A. Immune response to microsporidia. *Exp. Suppl.* **114**, 373–388 (2022).
12. Fischer, J., Suire, C. & Hale-Donze, H. Toll-like receptor 2 recognition of the microsporidia *Encephalitozoon* spp. induces nuclear translocation of NF-kappaB and subsequent inflammatory responses. *Infect. Immun.* **76**, 4737–4744 (2008).
13. Lawlor, E. M., Moretto, M. M. & Khan, I. A. Optimal CD8 T-cell response against *Encephalitozoon cuniculi* is mediated by Toll-like receptor 4 upregulation by dendritic cells. *Infect. Immun.* **78**, 3097–3102 (2010).
14. Moretto, M. M., Harrow, D. I., Hawley, T. S. & Khan, I. A. Interleukin-12-producing CD103+ CD11b- CD8+ dendritic cells are responsible for eliciting gut intraepithelial lymphocyte response against *Encephalitozoon cuniculi*. *Infect. Immun.* **83**, 4719–4730 (2015).
15. Moretto, M. M., Weiss, L. M., Combe, C. L. & Khan, I. A. IFN-γ-producing dendritic cells are important for priming of gut intraepithelial lymphocyte response against intracellular parasitic infection. *J. Immunol.* **179**, 2485–2492 (2007).
16. Khan, I. A., Schwartzman, J. D., Kasper, L. H. & Moretto, M. CD8+ CTLs are essential for protective immunity against *Encephalitozoon cuniculi* infection. *J. Immunol.* **162**, 6086–6091 (1999).
17. Moretto, M. M., Harrow, D. I. & Khan, I. A. Effector CD8 T cell immunity in microsporidial infection: a lone defense mechanism. *Semin. Immunopathol.* **37**, 281–287 (2015).
18. Braunfuchsová, P., Salát, J. & Kopecký, J. CD8+ T lymphocytes protect SCID mice against *Encephalitozoon cuniculi* infection. *Int. J. Parasitol.* **31**, 681–686 (2001).
19. Bhadra, R. et al. Intrinsic TGF-β signaling promotes age-dependent CD8+ T cell polyfunctionality attrition. *J. Clin. Invest.* **124**, 2441–2455 (2014).
20. Moretto, M. M. & Khan, I. A. IL-21 is important for induction of KLRG1+ effector CD8 T cells during acute intracellular infection. *J. Immunol.* **196**, 375–384 (2016).
21. Moretto, M., Casciotti, L., Durell, B. & Khan, I. A. Lack of CD4+ T cells does not affect induction of CD8+ T-cell immunity against Encephalitozoon cuniculi infection. *Infect. Immun.* **68**, 6223–6232 (2000).
22. Luo, G., Gao, Q., Zhang, S. & Yan, B. Probing infectious disease by single-cell RNA sequencing: progresses and perspectives. *Comput. Struct. Biotechnol. J.* **18**, 2962–2971 (2020).
23. Dooley, N. L., et al. Single cell transcriptomics shows that malaria promotes unique regulatory responses across multiple immune cell subsets. *Nat. Commun.* **14**, 7387 (2023).
24. Wilk, A. J. et al. A single-cell atlas of the peripheral immune response in patients with severe COVID-19. *Nat. Med.* **26**, 1070–1076 (2020).
25. Yang, X., et al. Single-cell profiling reveals distinct immune response landscapes in tuberculous pleural effusion and non-TPE. *Front. Immunol.* **14**, 1191357 (2023).
26. Scholzen, T. & Gerdes, J. The Ki-67 protein: from the known and the unknown. *J. Cell Physiol.* **182**, 311–322 (2000).
27. Rubin, C. I. & Atweh, G. F. The role of stathmin in the regulation of the cell cycle. *J. Cell Biochem.* **93**, 242–250 (2004).
28. Iyer, S. S. et al. Identification of novel markers for mouse CD4+ T follicular helper cells. *Eur. J. Immunol.* **43**, 3219–3232 (2013).
29. Meckiff, B. J. et al. Imbalance of regulatory and cytotoxic SARS-CoV-2-reactive CD4(+) T cells in COVID-19. *Cell.***183**, 1340-1353.e16 (2020).
30. Kumar, S. et al. Specialized Tfh cell subsets driving type-1 and type-2 humoral responses in lymphoid tissue. *Cell Discov.* **10**, 64 (2024).
31. Gounari, F. & Khazaie, K. TCF-1: a maverick in T cell development and function. *Nat. Immunol.* **23**, 671–678 (2022).
32. Escobar, G., Mangani, D. & Anderson, A. C. T cell factor 1: a master regulator of the T cell response in disease. *Sci. Immunol.* **5**, (2020). eabb9726.
33. Chen, Z. et al. TCF-1-centered transcriptional network drives an effector versus exhausted CD8 T cell-fate decision. *Immunity.***51**, 840–855.e5 (2019).
34. Hou, J. et al. ZC3H15 promotes gastric cancer progression by targeting the FBXW7/c-Myc pathway. *Cell Death Discov.* **8**, 32 (2022).
35. Cibrián, D. & Sánchez-Madrid, F. CD69: from activation marker to metabolic gatekeeper. *Eur. J. Immunol.* **47**, 946–953 (2017).
36. Xu, W. et al. The transcription factor Tox2 drives T follicular helper cell development via regulating chromatin accessibility. *Immunity* **51**, 826–839.e825 (2019).
37. Moretto, M., Durell, B., Schwartzman, J. D. & Khan, I. A. γδ T cell-deficient mice have a down-regulated CD8+ T cell immune response against *Encephalitozoon cuniculi* infection. *J. Immunol.* **166**, 7389–7397 (2001).
38. Saravia, J., Chapman, N. M. & Chi, H. Helper T cell differentiation. *Cell Mol. Immunol.* **16**, 634–643 (2019).
39. Sun, L., Su, Y., Jiao, A., Wang, X. & Zhang, B. T cells in health and disease. *Signal Transduct. Target Ther.* **8**, 235 (2023).

40. Chitu, V. & Stanley, E. R. Colony-stimulating factor-1 in immunity and inflammation. *Curr. Opin. Immunol.* **18**, 39–48 (2006).
41. Becher, B., Tugues, S. & Greter, M. GM-CSF: from growth factor to central mediator of tissue inflammation. *Immunity* **45**, 963–973 (2016).
42. Fontana, M. F. et al. Macrophage colony stimulating fctor derived from CD4+ T cells contributes to control of a blood-borne infection. *PLoS Pathog.* **12**, e1006046 (2016).
43. Mamedov, M. R. et al. A macrophage colony-stimulating-factor-producing γδ T cell subset prevents malarial parasitemic recurrence. *Immunity* **48**, 350–363.e357 (2018).
44. Didier, E. S. et al. Reactive nitrogen and oxygen species, and iron sequestration contribute to macrophage-mediated control of *Encephalitozoon cuniculi* (Phylum Microsporidia) infection in vitro and in vivo. *Microbes Infect.* **12**, 1244–1251 (2010).
45. Lu, Y. et al. *Encephalitozoon hellem* infection promotes monocytes extravasation. *Pathogens* **11**, 914 (2022).
46. Salát, J., Sak, B., Le, T. & Kopecký, J. Susceptibility of IFN-γor IL-12 knock-out and SCID mice to infection with two microsporidian species, *Encephalitozoon cuniculi* and *E. intestinalis*. *Folia Parasitol. (Praha)* **51**, 275–282 (2004).
47. Belyaev, N. N., Biró, J., Langhorne, J. & Potocnik, A. J. Extramedullary myelopoiesis in malaria depends on mobilization of myeloid-restricted progenitors by IFN-γ induced chemokines. *PLoS Pathog.* **9**, e1003406 (2013).
48. Belyaev, N. N. et al. Induction of an IL7-R+c-Kithi myelolymphoid progenitor critically dependent on IFN-γ signaling during acute malaria. *Nat. Immunol.* **11**, 477–485 (2010).
49. Omilusik, K. D. et al. Transcriptional repressor ZEB2 promotes terminal differentiation of CD8+ effector and memory T cell populations during infection. *J. Exp. Med.* **212**, 2027–2039 (2015).
50. Chowdhury, D. & Lieberman, J. Death by a thousand cuts: granzyme pathways of programmed cell death. *Annu. Rev. Immunol.* **26**, 389–420 (2008).
51. Kelso, A. et al. The genes for perforin, granzymes A-C and IFN-γ are differentially expressed in single CD8+ T cells during primary activation. *Int. Immunol.* **14**, 605–613 (2002).
52. Zhou, Z. et al. Granzyme A from cytotoxic lymphocytes cleaves GSDMB to trigger pyroptosis in target cells. *Science* **368**, eaaz7548 (2020).
53. Susanto, O. et al. Mouse granzyme A induces a novel death with writhing morphology that is mechanistically distinct from granzyme B-induced apoptosis. *Cell Death Differ.* **20**, 1183–1193 (2013).
54. Ewen, C. L., Kane, K. P. & Bleackley, R. C. A quarter century of granzymes. *Cell Death Differ.* **19**, 28–35 (2012).
55. Chora, Â, et al. Interplay between liver and blood stages of *Plasmodium* infection dictates malaria severity via γδ T cells and IL-17-promoted stress erythropoiesis. *Immunity* **56**, 592–605.e598 (2023).
56. Wang, T. et al. γδ T cells facilitate adaptive immunity against West Nile virus infection in mice. *J. Immunol.* **177**, 1825–1832 (2006).
57. Lees, R. K., Ferrero, I., Fau, -, MacDonald, H. R. & MacDonald, H. R. Tissue-specific segregation of TCRgamma delta+ NKT cells according to phenotype TCR repertoire and activation status: parallels with TCR alphabeta+NKT cells. *Eur. J. Immunol.* **31**, 2901–2909 (2001).
58. Pavie, J. et al. Prevalence of opportunistic intestinal parasitic infections among HIV-infected patients with low CD4 cells counts in France in the combination antiretroviral therapy era. *Int. J. Infect. Dis.* **16**, e677–e679 (2012).
59. Moretto, M., Weiss, L. M. & Khan, I. A. Induction of a rapid and strong antigen-specific intraepithelial lymphocyte response during oral *Encephalitozoon cuniculi* infection. *J. Immunol.* **172**, 4402–4409 (2004).
60. Salat, J., Braunfuchsová, P., Kopecký, J. & Ditrich, O. Role of CD4+ and CD8+ T lymphocytes in the protection of mice against *Encephalitozoon intestinalis* infection. *Parasitol. Res.* **88**, 603–608 (2002).
61. Quan, Y. Z. et al. Reprogramming by drug-like molecules leads to regeneration of cochlear hair cell-like cells in adult mice. *Proc. Natl. Acad. Sci. USA* **120**, (2023). e2215253120.
62. Tsuchiya, Y., et al. Fibroblast growth factor 18 stimulates the proliferation of hepatic stellate cells, thereby inducing liver fibrosis. *Nat. Commun.* **14**, 6304 (2023).
63. Godoy, R. S. et al. Single-cell transcriptomic atlas of lung microvascular regeneration after targeted endothelial cell ablation. *Elife* **12**, e80900 (2023).
64. Butler, A., Hoffman, P., Smibert, P., Papalexi, E. & Satija, R. Integrating single-cell transcriptomic data across different conditions, technologies, and species. *Nat. Biotechnol.* **36**, 411–420 (2018).
65. Stuart, T. et al. Comprehensive integration of single-cell data. *Cell* **177**, 1888–1902.e1821 (2019).
66. McGinnis, C. S., Murrow, L. M. & Gartner, Z. J. DoubletFinder: doublet detection in single-cell RNA sequencing data using artificial nearest neighbors. *Cell Syst.* **8**, 329–337.e324 (2019).
67. Zhang, X. et al. CellMarker: a manually curated resource of cell markers in human and mouse. *Nucleic Acids Res.* **47**, D721–D728 (2019).
68. Camp, J. G. et al. Multilineage communication regulates human liver bud development from pluripotency. *Nature* **546**, 533–538 (2017).

Acknowledgements

This work was supported by the National Natural Science Foundation of China (No. 31802141); Fundamental Research Funds for the Central Universities (XDJK2020B005, SWU-XDJH202322).

Author contributions

Yunlin Tang: Conceptualization, experiment design, data analysis, validation, visualization, methodology, data curation, software, writing-original draft, review & editing; Lu Cao: Experiment, data analysis, validation, methodology; Jiangyan Jin: Experiment, data analysis; Tangxin Li: Experiment, data analysis; Yebo Chen: Experiment, data analysis, validation; Yishan Lu: Experiment, data analysis; Tian Li: Data curation, validation, supervision, resources; Louis M. Weiss: Conceptualization, resources, supervision; Guoqing Pan: Conceptualization, supervision, project administration; Jialing Bao: Conceptualization, supervision, methodology, project administration, data curation, resources, writing-original draft, review & editing, funding acquisition; Zeyang Zhou: Conceptualization, supervision, project administration, funding acquisition.

Competing interests

The authors declare no competing interests.

Additional information

Supplementary information The online version contains supplementary material available at https://doi.org/10.1038/s42003-025-07990-4.

Correspondence and requests for materials should be addressed to Jialing Bao or Zeyang Zhou.

Peer review information *Communications Biology* thanks Pattana Jaroenlak and the other, anonymous, reviewer(s) for their contribution to the peer review of this work. Primary Handling Editor: Johannes Stortz.